Bioorganic & Medicinal Chemistry 17 (2009) 2623–2631

Contents lists available at ScienceDirect

Bioorganic & Medicinal Chemistry

journal homepage: www.elsevier.com/locate/bmc

# Exploration and synthesis of curcumin analogues with improved structural stability both in vitro and in vivo as cytotoxic agents

Guang Liang [a,b], Lili Shao [b], Yi Wang [b], Chengguang Zhao [b], Yanhui Chu [c], Jian Xiao [b], Yu Zhao [b], Xiaokun Li [a,b,*], Shulin Yang [a,*]

[a] College of Chemical Engineering, Nanjing University of Science and Technology, 200 Xiaolingwei St., Nanjing, Jiangsu 210094, China
[b] School of Pharmacy, Wenzhou Medical College, 1210 College Town, Wenzhou, Zhejiang 325035, China
[c] Heilongjiang Province Key Laboratory of Anti-fibrosis Biotherapy, Mudanjiang Medical College, Mudanjiang, Heilongjiang 157011, China

ARTICLE INFO

*Article history:*
Received 13 September 2008
Revised 17 October 2008
Accepted 18 October 2008
Available online 1 November 2008

*Keywords:*
Curcumin analogues
Stability
Pharmacokinetics
Cytotoxic activity
Structure–activity relation

ABSTRACT

Curcumin has a surprisingly wide range of chemo-preventive and chemo-therapeutic activities and is under investigation for the treatment of various human cancers. However, the clinical application of curcumin has been significantly limited by its instability and poor metabolic property. Although a number of synthetic modifications of curcumin have been studied intensively in order to develop a molecule with enhanced bioactivities, few synthetic studies were done for the improvement of pharmacokinetic profiles. In the present study, a series of mono-carbonyl analogues of curcumin were designed and synthesized by deleting the reactive β-diketone moiety, which was considered to be responsible for the pharmacokinetic limitation of curcumin. The results of the in vitro stability studies and in vivo pharmacokinetic studies indicated that the stability of these mono-carbonyl analogues was greatly enhanced in vitro and their pharmacokinetic profiles were also significantly improved in vivo. Furthermore, the cytotoxic activities of mono-carbonyl analogues were evaluated in seven different tumor cell lines by MTT assay and the structure–activity relation (SAR) was discussed and concluded. The results suggest that the five-carbon linker-containing analogues of curcumin may be favorable for the curcumin-based drug development both pharmacokinetically and pharmacologically.



## 1. Introduction

Curcumin [1,7-bis-(4-hydroxy-3-methoxyphenyl)-1,6-heptadiene-3,5-dione] is a yellow compound isolated from the rhizome of the herb *Curcuma longa L.*, which has been used for centuries as a dietary pigment, spice, and traditional medicine in India and China.[1,2] Recent clinical studies reported that curcumin could be orally administered up to 12 g/day without any toxic effect in humans.[3] During the last two decades, numerous studies have shown that curcumin possesses multifunctional pharmacological properties including inducing apoptosis in a variety of tumor cells.[4–9] Several clinical trials of curcumin are currently conducted in patients with pancreatic cancer, multiple myeloma, rheumatoid arthritis, cystic fibrosis, inflammatory bowel disease, psoriasis, and other disorders.[10]

Although curcumin is remarkably non-toxic and has promising anti-inflammation and anti-cancer activities, preclinical and clinical studies indicate that its poor bioavailability and pharmacokinetic profiles due to its instability under physiological conditions have limited its application in anti-cancer therapies.[10–12] For example, in a phase I trial, the concentrations of curcumin in plasma and target tissues were as low as 11.1 nM and 1.3 μM, respectively, even with an oral administration of 3.6 g/day[12,13] Evidences from both in vitro and in vivo studies show that the β-diketone moiety is responsible for the instability and weak pharmacokinetic profiles of curcumin.[14] In vitro, curcumin is unstable at a pH above 6.5 because of the highly reactive β-diketone moiety in the structure of curcumin.[15,16] And in vivo, recent studies indicate that the β-diketone moiety appears to be a specific substrate of a series of aldo-keto reductases[17–19] and can be decomposed rapidly (Fig. 1).

During the last decade, synthetic modifications of curcumin, which were aimed at enhancing its bioactivities, have been intensively studied. However, few of these studies were focused on the improvement of its pharmacokinetic profiles. It is suggested that the stability and metabolic profiles of curcumin could be enhanced by deleting the β-diketone moiety. Although previous studies suggest that the presence of the β-diketone moiety may be necessary for the biological activities of curcumin, recent studies from several independent groups demonstrated that some curcumin analogues containing a 5-carbon enone spacer without β-diketone either retained or increased growth-suppressive activities against several

* Corresponding authors. Tel./fax: +86 25 84315945.
*E-mail addresses:* cuiliang1234@163.com (X. Li), bioshuliny@yahoo.com.cn (S. Yang).

0968-0896/$ - see front matter © 2009 Published by Elsevier Ltd.
doi:10.1016/j.bmc.2008.10.044

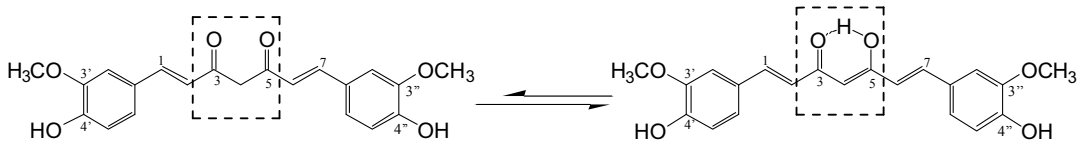


**Figure 1.** Chemical structure of curcumin, where the α,β-unsaturated β-diketone (heptadiene-dione) moiety, undergoing keto-enol tautomerism and forming a hydrogen bond-containing 6-membered ring, may play a important role in the instability and weak pharmacokinetic profile of curcumin.

cancer cells.[20,21] Our previous studies also showed that some mono-carbonyl analogues of curcumin without the β-diketone moiety exhibited better anti-bacterial[22] and anti-inflammatory[23] activities than those of curcumin. In the present study, we designed and synthesized a series of β-diketone-excluding mono-carbonyl analogues of curcumin which exhibited enhanced stability in vitro and greatly improved pharmacokinetic profiles in vivo. Further in vitro cell-killing evaluation in seven different cancer cells showed that some analogues possessed higher cytotoxic activities than that of their leading compound. We also discussed the possible cytotoxic structure–activity relation (SAR) of these 5-carbon spacer-containing analogues using three different 5-carbon linkers: cyclopentanone (**A**), acetone (**B**), and cyclohexanone (**C**) and various substitutes on the aryl rings.

## 2. Results and discussion

### 2.1. Chemistry

As we previously reported,[22] the synthesis of compounds **1** and **2** (shown in Fig. 2) started from the protection of 4-hydroxybenzaldehyde with tetrahydropyran-2-yl to afford protected compounds. Compounds **14** and **16** were synthesized by aldol condensation of the protected compound with acetone (**B**), cyclopentanone (**A**), and cyclohexanone (**C**). Compounds **1** (or **2**) were subsequently obtained by hydrolysis of **14** (or **15**) using a catalytic amount of *p*-toluenesulfonic acid and compounds **11** (or **10**) were obtained by further etherification with allyl bromide. Other compounds were synthesized by direct coupling of *p*-fluorobenzaldhyde with the three ketones in alkaline media (shown in Fig. 2). The synthesis and structures of heterocyclic analogues are shown in Table 3. The yield, melt point, and spectral analysis in $^1$H NMR and MS of these compounds are shown in Section 4. The diaryl structure is confirmed by the absence of methyl protons in the $^1$H NMR spectra of **A**-class compounds and the absence of two methylene protons in the spectra of **B-** and **C-**class compounds.

### 2.2. Stability of analogues in vitro

The hydrolytic stabilities of the curcumin analogues were investigated in buffered 0.3% CMCNa solution at pH 7.4 and 37 °C in sodium dihydrogen phosphate buffer. The data shown in Figure 3 represent the distribution of the degradation degree of curcumin and 20 analogues after being kept in buffer for 75 h. In the conditions above, more than 64% of curcumin degraded, while all of the analogues degraded much less than curcumin with different distribution on a scale of 0–60%. Four compounds still retained more than 90% of the original content after 75 h in pH 7.4 buffer. In a recent report, Wang and coworkers[15] found that 92% of curcumin degraded when added to a 0.1 M phosphate buffer with pH 7.2 for 30 min. Tomren[16] also showed a half-life of 10.5 h when curcumin was kept in pH 8.0 buffer containing 10% cyclodextrins. It can be postulated that the hydrolytic degradation starts with an attack from the nucleophilic $OH^-$ ion on the carbonyl carbon in the keto-enol form of the β-diketone moiety in curcumin. The main hydrolytic degradation products and mechanisms have been identified previously.[15] Our data showed that the analogues lacking the β-diketone moiety were much more stable in the pH 7.4 situation. As a result, the stability of curcumin could be enhanced through deleting the β-diketone moiety.

### 2.3. Pharmacokinetic profiles of analogues in vivo

The in vivo pharmacokinetic data showed improved pharmacokinetic profiles of our β-diketone-deleted analogues of curcumin. We used the compound **B02**, which only lacks the β-diketone in the structure compared with curcumin, **B33** and curcumin for pharmacokinetic study in rats. After oral administration at a dose of 500 mg/kg, respectively, 0.5 ml blood was obtained from fossa orbitalis veniplex of rats at 0.083, 0.25, 0.5, 1, 2, 4, and 8 h. HPLC was used to determine the concentration of each compound in plasma and the DAS software was used for the non-compartmental pharmacokinetic analysis of the plasma concentration–time data. The detailed chromatographic conditions, HPLC methodology, linearity, accuracy, and precision are shown in the Supplemental file. The methodological data showed excellent chromatographic specificity and no interference from blank plasma in these three compounds (shown in Figure S1). The calibration curves of three compounds were presented in Figure S2 with coefficient of correlation $R_2 = 0.9998$ (curcumin), 0.9997 (**B02**), and 0.9992 (**B33**). Good inter-day and intra-day precision (SD < 5% in all concentration, $n = 3$) and high extraction efficiency (recovery > 95%, $n = 3$) were shown in Tables S1 and S2.

The mean (±SD) plasma concentration–time curves of curcumin, **B02** and **B33** in the plasma of healthy rats ($n = 4$) are shown in Figure 4. The pharmacokinetic parameters were presented in Table 1. With 500 mg/kg oral administration, the peak concentration of curcumin reached only 0.091 μg/ml and decreased to as low as 0.04 μg/ml 2 h after administration. The deletion of β-diketone enhanced the peak concentration of **B02** to 0.82 μg/ml, and **B33**, the 2′-bromo substituted mono-carbonyl reach a much higher plasma concentration of 4.1 μg/ml. Furthermore, there was an apparent decrease of clearance (CL) comparing curcumin (835.2 L/kg/h) with **B02** (125.4 L/kg/h) and **B33** (38.98 L/kg/h). The differences in the total amount of compounds in plasma, represented by the area under the curve (AUC), also exhibited large increases from curcumin to mono-carbonyl analogues. Additionally, the half-life of **B02** was increased twice more than that of curcumin; and there was a quick absorption of compound **B33**. In summary, our results in pharmacokinetics indicate, to some extent, that the deletion of β-diketone significantly decreases the degree and speed of metabolism of curcuminoids, and the mono-carbonyl analogues of curcumin may possess much better pharmacokinetic profiles than curcumin.

### 2.4. Cytotoxic properties against tumor cells and structure–activity relation (SAR)

It has been reported that curcumin possesses a wide-spectrum of anti-tumor properties.[4–9] The cytotoxicity against seven human tumor cell lines of present mono-carbonyl analogues, including

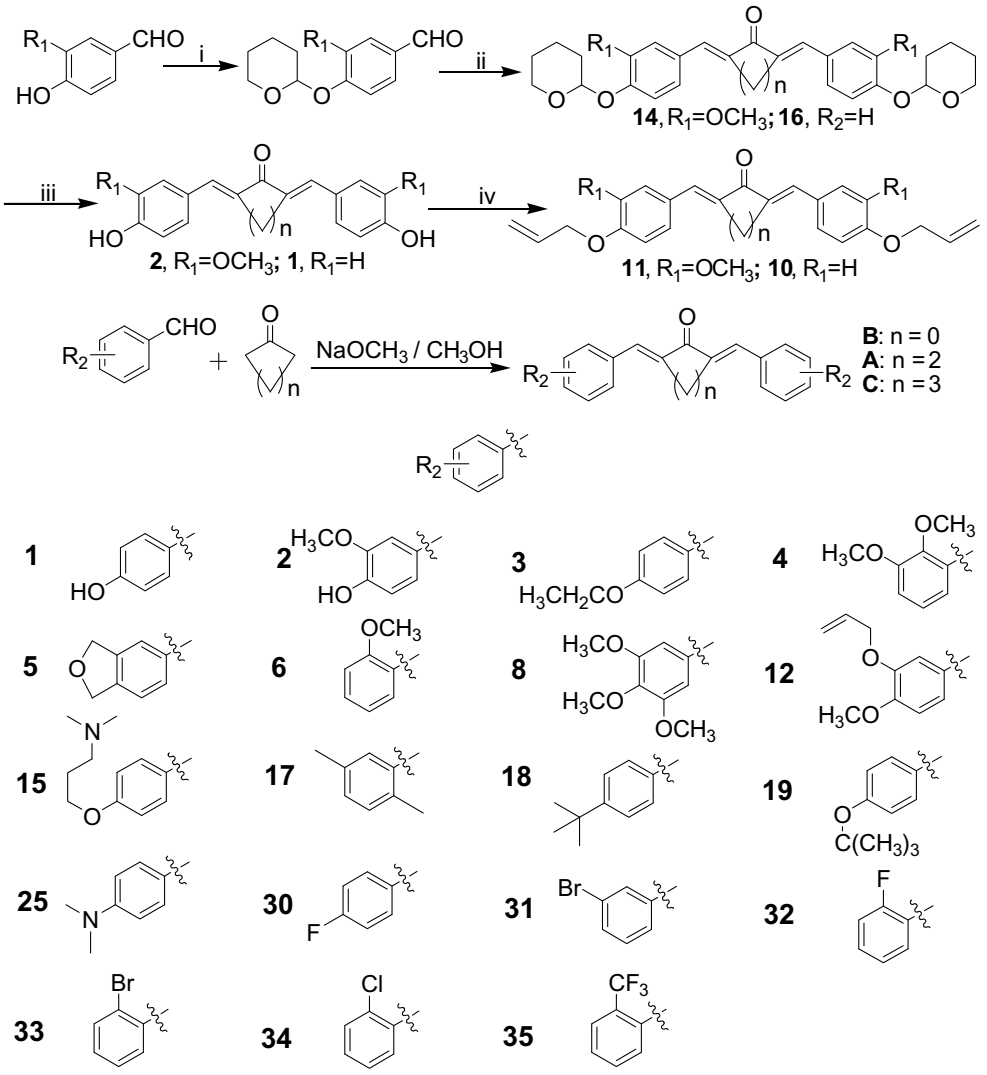


**Figure 2.** Structures and synthesis of present compounds. Reagents and conditions: (i) 3,4-dihydro-α-pyran, pyridine–PTSA, $CH_2Cl_2$, rt; (ii) acetone, cyclopentanone or cyclohexanone, NaOH/EtOH, rt; (iii) PTSA, MeOH, rt; (iv) allylbromide, $K_2CO_3$/acetone, reflux.

BGC823, CNE, HL-60, KB, LS174T, PC3, and HeLa (shown in Table 2 and 3) were evaluated using the MTT method. Most of the benzene ring-containing compounds exhibited anti-proliferation activities against selected tumor cells (shown in Table 2).

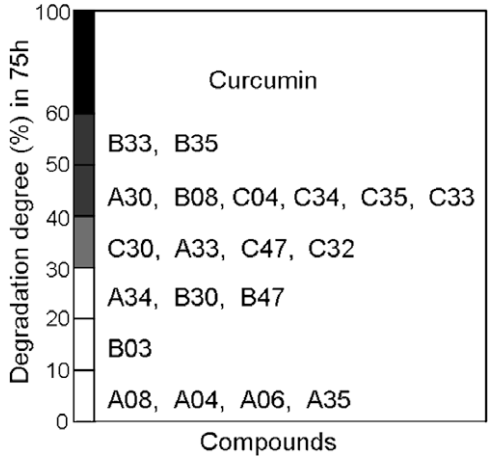


**Figure 3.** The distribution of degradation rate of curcumin analogues after incubation in pH 7.4 phosphate buffer at 37 °C for 75 h.

It could be concluded from Table 2 that **B**-class and **C**-class compounds possessed much higher activities than the **A**-class ones did. For example, there were 18 inactive compounds ($IC_{50}$ > 100 μM) in **A**-class with 2 in **B**-class and 4 in **C**-class (data not shown). Either the acetone or cyclohexanone spacer maintained or increased the cell-killing activity while the cyclopentanone decreased it, which indicates that the different structures in the central spacer may play an important role in the cytotoxic properties. In our previous paper,[24] we considered that the presence of cyclohexanone in **C**-class compound, which remotely resembles the 6-membered ring in the enol tautomer in curcumin, may play an important role in the anti-inflammatory activities by analyzing and comparing the data of single-crystal X-ray diffraction of **C30** and curcumin. Now, we also think the similarity between the cyclohexanone spacer and the enol tautomer 6-membered ring is, at least partly, the reason why **C**-class compounds possess higher bioactivities than **A**-class compounds do. In addition, curcumin exists in two tautomers: enol form and ketone form. The fact that the **B**-class compounds without ring spacers exhibit excellent anti-tumor properties indicates that the ketone form also contributes to the cytotoxic potential of curcumin.

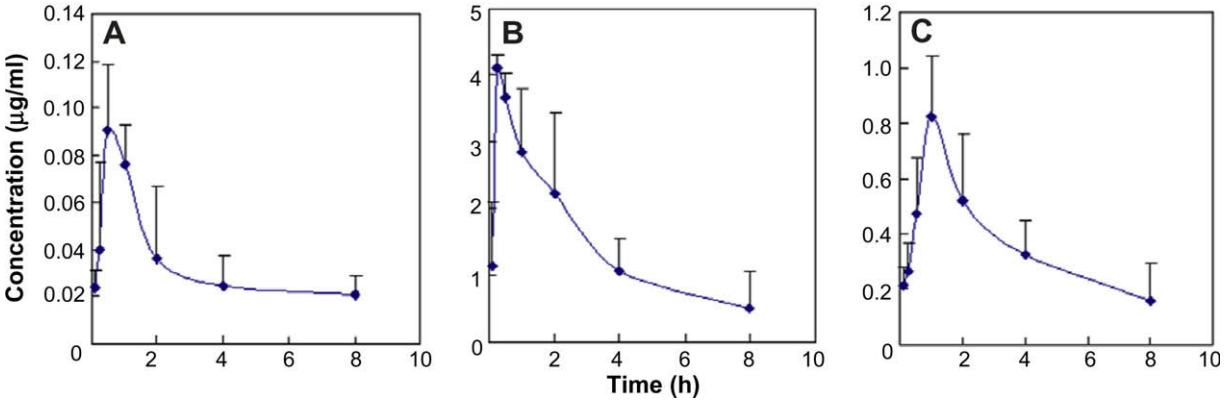


**Figure 4.** Mean (±SD) plasma concentration–time profiles of curcumin (A), **B33** (B), and **B02** (C) in the plasma of healthy rats ($n = 4$), which were administered a single oral dose of 500 mg compound per kg of body weight.

**Table 1**
Pharmacokinetic characteristics of curcumin, **B2** and **B33** in the plasma of healthy rats ($n = 4$) that were administrated a single oral dose of 500 mg compound per kg of body weight.

| Parameters | Curcumin | B33 | B2 |
|---|---|---|---|
| $AUC_{0-t}$ (mg h/L) | 0.275 ± 0.236 | 12.053 ± 4.34 | 2.964 ± 1.004 |
| $AUC_{0-\infty}$ (mg h/L) | 0.672 ± 0.218 | 14.907 ± 7.31 | 4.913 ± 2.896 |
| $t_{1/2}$ (h) | 2.412 ± 1.80 | 2.92 ± 1.3 | 5.964 ± 4.314 |
| $MRT_{0-t}$ (h) | 3.436 ± 0.667 | 2.486 ± 0.53 | 2.959 ± 0.476 |
| $MRT_{0-\infty}$ (h) | 22.693 ± 16.16 | 4.157 ± 2.06 | 8.478 ± 5.866 |
| CL (L/kg/h) | 835.23 ± 379.4 | 38.98 ± 17.16 | 125.422 ± 55.969 |
| $C_{max}$ (μg/ml) | 0.091 ± 0.12 | 4.1 ± 0.19 | 0.822 ± 0.219 |
| $T_{max}$ (h) | 0.50 | 0.25 | 1.00 |

Among the compounds containing 4′-OH, **02** compounds with 3′-$OCH_3$-4′-OH possessed much stronger cytotoxicity than **01** compounds with a single 4′-OH did. For example, **B01** exhibited low cytotoxicity against KB, PC3, and Hela cells with high $IC_{50}$ value (>40 μM), while the $IC_{50}$ of **B02** against CNE and LS174T reached 6.8 and 3.7 μM; **C01** was inactive against all seven kinds of tumor cells but **C02** showed good inhibitory activities against CNE, KB, and LS174T cells. The cell-killing effects of both **B02** and **C02** were stronger than that of the leading curcumin. Previous reports[25,26] also showed the formation of hydrogen bonding between 3′-$OCH_3$ and 4′-OH of curcumin decreased the electron-donating ability of 4′-OH. Thus, our data suggest that reduction of the electron-donating ability of the 4′-substituent may increase the bioactivities of mono-carbonyl analogues.

Alkylation is a common approach to reduce the electron-donating ability of OH. Lin and his coworkers found that 1,5-bis(3′,4′-dimethoxyphenyl)penta-1,4-dien-3-one, dimethoxy **B02**, possessed a high anti-proliferation effect against PC3 and LNCaP cells with an $IC_{50} < 5.0$ μM.[28] From the data in Table 2, the conclusion that a weak electron-donating substitute in the 4′-position may increase the inhibitory activity against tumor cells is reinforced. For instance, (1) 3′,4′,5′-trimethoxy substituted compounds **B08** and **C08** exhibited broad-spectral cytotoxic activities and the $IC_{50}$ value of **B08** to PC3 reached 8.8 μM, lower than those of curcumin and cisplatin; (2) the alkylation of **C01** using allyl bromide led to **C10** killing KB cells; (3) the 4′-ethoxyl compounds **3** showed cytotoxicity, especially **C03** with an $IC_{50}$ = 5.6 μM against LS174T; (4) **B16**, the compound from alkylized **B01** by tetrahydro-2*H*-pyran-2-yl, exhibited the lowest $IC_{50}$ value (0.3 μM towards HL-60) among all of present compounds; (5) with the negative effect of cyclopentanone, **A12**, **A05**, and **A15**, however, still showed excellent cytotoxic activities, especially **A15** with $IC_{50}$ = 2.4 μM towards CNE and 3.3 μM towards KB. In addition, the strongly electron-donating 4′-(*N*,*N*-dimethylamino) compound **B25** showed no cytotoxic activity while the weakly electron-donating 4′-*tert*-butyl compound **B18** exhibited an $IC_{50}$ value against PC3 that was lower than those of curcumin and cisplatin. Without the electron-effective moiety in the 4′-position, compounds **04**, **17**, and **06** also exhibited excellent cytotoxic properties. For example, the $IC_{50}$ values of **B04** (against HL-60), **B17** (against PC3 and HeLa), and **A06** (against HL-60 and PC3) were all below 10 μM, lower than those of curcumin and cisplatin. We also analyzed the change of cytotoxicity when an electron-withdrawing moiety occupied the 4′-position of analogues. Both **B30** and **C30** with the 4′-F substitute exhibited broad-spectra cytotoxicity, but with relatively high $IC_{50}$ values. Over all, the analysis of the 4′-position substitutes shows that the cytotoxic activity of mono-carbonyl analogues: could be increased by occupying the 4′-position with a weak electron-donating substitute or a hydrogen atom, could be reduced through the induction of a strong electron-withdrawing substitute and could be lost by the import of a strong electron-donating substitute.

The electron-withdrawing halogens were used to analyze the role of a substitute at the 2′-position towards cytotoxic activity. **B33** (2′-Br), **C34** (2′-Cl), and **C32** (2′-F) showed broad-spectra cytotoxicity, and the $IC_{50}$ of five of the 2′-halogen substituted were lower than 10 μM. The anti PC3 effect of **B35** (2′-$CF_3$) reached the highest with $IC_{50}$ of 0.4 μM compared with any other tested compounds. Thus, our data indicate that the electron-withdrawing substitution at the 2′-position could enhance the cytotoxic activity. In addition, by comparing the activities of **B33**, **B06**, **B34**, and **B35**, we can conclude that the stronger the electronegativity of the 2′-substituent, the stronger the cytotoxicity against tumor cells.

Recent studies[27,28] showed that the benzene in the structure of curcumin was not the unique aromatic ring for the bioactivity. We also evaluated the cytotoxic properties of mono-carbonyl analogues containing other aromatic rings (shown in Table 3). Among these compounds, both **B40** with a furan ring and **B41** with a thiophene ring were broad-spectra cytotoxic compounds. **A44** and pyrrole-containing **A45** exhibited strong inhibition against LS174T. The $IC_{50}$ value of **C45** towards KB cells reached 2.3 μM, which was much lower than that of curcumin. And the analogues containing styryl and naphtalin also exhibited inhibitory activities against different tumor cells. Thus, our data indicate that the substitution of benzene by other aromatic rings may maintain or enhance the cytotoxic activities of mono-carbonyl analogues of curcumin.

In summary, the SAR analysis of mono-carbonyl analogues of curcumin is shown in Figure 5. At 2′-position, a strong electron-withdrawing substituent may increase bioactivity and the more

**Table 2**
Structure and cytotoxicity of present compounds against seven tumor cells.

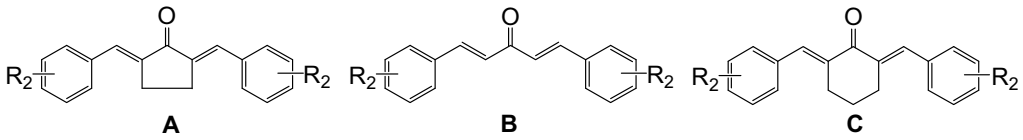


| Compound | R | $IC_{50}$ μmol/L | | | | | | |
|---|---|---|---|---|---|---|---|---|
| | | BGC 823 | CNE | HL-60 | KB | LS 174T | PC3 | HeLa |
| **A3** | 4′-$OCH_2CH_3$ | | | | | | | 24.0 ± 3.9 |
| **A4** | 2′-$OCH_3$-3′-$OCH_3$ | | | | | | | 249 ± 54.0 |
| **A5** | 3′,4′-(O-$CH_2$-O) | | | 225 ± 47.1 | | | | |
| **A6** | 2′-$OCH_3$ | | | 2.3 ± 0.9 | | | 5.3 ± 2.0 | |
| **A8** | 3′,4′,5′-$(OCH_3)_3$ | | | | | | | |
| **A12** | 3′-($OCH_2CHCH_2$)-4′-$OCH_3$ | 32.6 ± 6.6 | | | | | | |
| **A15** | 4′-$OCH_2CH_2CH_2N(CH_3)_2$ | | 2.4 ± 1.5 | | 3.3 ± 1.8 | | | |
| **A16** | 4′-(Tetrahydro-2*H*-pyran-2-yl)oxy | | | | | | | 39.1 ± 7.0 |
| **A25** | 4′-$N(CH_3)_2$ | | | | | | | |
| **A30** | 4′-F | | | | | | | 1.2 ± 0.3 |
| **A33** | 2′-Br | | 32.8 ± 5.0 | | 109 ± 15.8 | | 24.7 ± 4.4 | |
| **A34** | 2′-Cl | | | 87.2 ± 18.7 | 96.0 ± 26.6 | | | |
| **A35** | 2′-$CF_3$ | | | | <9.34 | 213 ± 43.9 | | |
| **Bl** | 4′-OH | | | | 41.5 ± 11.6 | | 48.9 ± 9.2 | 217 ± 33.9 |
| **B2** | 3′-$OCH_3$-4′-OH | | 6.8 ± 1.6 | | | 3.7 ± 0.7 | | |
| **B4** | 2′-$OCH_3$-3′-$OCH_3$ | 24.4 ± 2.6 | | 4.5 ± 3.6 | 24.3 ± 3.9 | 48.0 ± 10.7 | | |
| **B6** | 2′-$OCH_3$ | | | <12.6 | <12.6 | | | 161 ± 42.3 |
| **B8** | 3′,4′,5′-$(OCH_3)_3$ | | | | 98.7 ± 15.0 | 148 ± 22.5 | 8.8 ± 1.1 | 95.0 ± 20.0 |
| **Bl0** | 4′-$OCH_2CH{=}CH_2$ | | | 64.6 ± 15.8 | | | | |
| **B16** | 4′-(Tetrahydro-2*H*-pyran-2-yl)oxy | | | 0.3 ± 0.16 | | | 43.4 ± 11.8 | |
| **B17** | 2′-$CH_3$-5′-$CH_3$ | | 17.7 ± 2.6 | | | 103 ± 19.3 | 5.2 ± 2.1 | 6.1 ± 1.0 |
| **B18** | 4′-$C(CH_3)_3$ | | 89.8 ± 24.0 | | | | 12.0 ± 2.9 | 21.8 ± 6.3 |
| **B30** | 4′-F | — | — | — | 94.6 ± 14.3 | 98.8 ± 19.1 | 15.2 ± 2.9 | |
| **B33** | 2′-Br | 16.1 ± 2.6 | | | | 4.0 ± 0.6 | 15.4 ± 6.0 | 34.2 ± 7.8 |
| **B34** | 2′-Cl | | | 8.6 ± 2.6 | 59.0 ± 12.0 | | | |
| **B35** | 2′-$CF_3$ | | | <10.0 | <3.70 | | 0.35 ± 0.1 | |
| **C2** | 3′-$OCH_3$-4′-OH | | 17.6 ± 6.9 | | <10.10 | 4.6 ± 2.5 | | |
| **C3** | 4′-$OCH_2CH_3$ | | | 85.8 ± 28.2 | | 5.6 ± 1.3 | | |
| **C4** | 2′-$OCH_3$-3′-$OCH_3$ | 55.3 ± 16.6 | | | 179 ± 67.0 | 84.5 ± 23.1 | | |
| **C8** | 3′,4′,5′-$(OCH_3)_3$ | | | 29.3 ± 7.4 | 117 ± 39.9 | | 22.7 ± 11.0 | 27.5 ± 10.1 |
| **Cl0** | 4′-$OCH_2CH{=}CH_2$ | | | | 85.3 ± 29.2 | | | |
| **Cll** | 3′-$OCH_3$-4′-$OCH_2CHCH_2$ | | | | 102 ± 40.6 | | | |
| **C16** | 4′-(Tetrahydro-2*H*-pyran-2-yl)oxy | | | 134 ± 44.7 | | 3.9 ± 0.8 | | |
| **C17** | 2′-$CH_3$-5′-$CH_3$ | | | | 35.3 ± 10.8 | | | |
| **C18** | 4′-$C(CH_3)_3$ | | | | 78.9 ± 25.6 | | | |
| **C30** | 4′-F | 87.3 ± 26.9 | 77.9 ± 20.7 | 58.1 ± 15.4 | 150 ± 41.3 | 7.4 ± 2.4 | | |
| **C31** | 3′-Br | | | | 15.9 ± 6.5 | 11.5 ± 3.6 | | 15.7 ± 7.4 |
| **C32** | 2′-F | | 130 ± 32.3 | | 74.1 ± 24.8 | | 45.8 ± 9.6 | 15.5 ± 3.1 |
| **C33** | 2′-Br | | | | 55.3 ± 14.6 | | | |
| **C34** | 2′-Cl | 4.4 ± 0.9 | | 98.3 ± 17.8 | 6.7 ± 1.5 | 4.2 ± 2.1 | 13.8 ± 3.2 | |
| **C35** | 2′-$CF_3$ | | | | 54.0 ± 19.9 | | | 46.3 ± 15.9 |
| Cur | Curcumin | 16.7 ± 2.3 | 32.8 ± 6.7 | 11.6 ± 0.9 | 35.9 ± 21.0 | 6.4 ± 1.0 | 15.0 ± 2.9 | 17.5 ± 2.2 |
| DDP | Cisplatin | 12.1 ± 2.0 | 5.0 ± 1.1 | 59.4 ± 18.2 | 3.1 ± 0.7 | 2.7 ± 1.3 | 19.6 ± 6.2 | 10.8 ± 3.8 |

electronegative the moiety is, the more cytotoxic the compound is. At the 4′-position, a weak electron-donating substituent is most favorable to the cytotoxic activity of the compound, a strong electron-donating moiety may remove the cytotoxic bioactivity and a strong electron-withdrawing one may reduce it. Towards the 5-carbon linker, the acetone and cyclohexanone spacers are much more favorable than the cyclopentanone one. And, the introduction of a heteroaromatic ring is also pharmacologically accessible.

None of our analogues can inhibit the growth of all seven tumor cells. It has been reported that curcumin exerts anti-cancer function through various pathways.[29] Therefore, the reduced anti-tumor spectra of analogues compared with curcumin may indicate a different molecular mechanism and targets between curcumin and analogues for inducing tumor cell apoptosis. The underlying molecular mechanism and the development of new anti-cancer analogues of curcumin are the focus of our continuing research.

## 3. Conclusion

The clinical application and development of curcumin have been limited by its instability and poor metabolic property. In this paper, we present a series of mono-carbonyl analogues of curcumin with enhanced stability in vitro and improved pharmacokinetic profiles in vivo. Subsequently, the cytotoxic activities of mono-carbonyl analogues against seven tumor cells were evaluated by MTT method. The SAR analysis found that curcumin analogues with the acetone or cyclohexanone spacer, 4′-weak electron-donating substitutes and 2′-electron-withdrawing substitutes are beneficial to increasing the cytotoxic activity. In addition,

**Table 3**
Synthesis, structures, and cytotoxicity of non-benzene aromatic ring analogues against seven tumor cells.

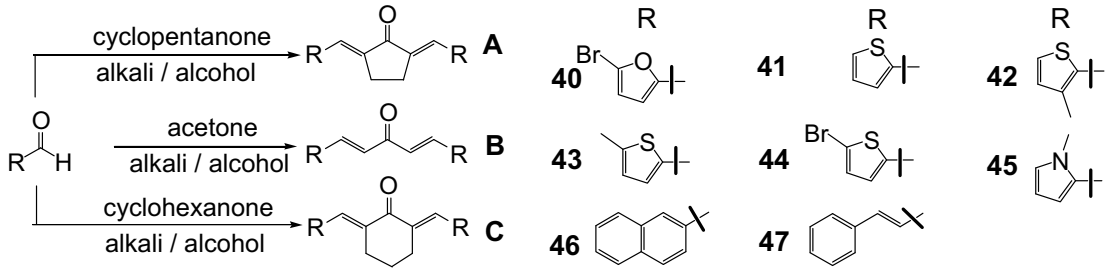


| Compound | $IC_{50}$ μg/ml | | | | | | |
|---|---|---|---|---|---|---|---|
| | BGC 823 | CNE | HL-60 | KB | LS 174T | PC3 | HeLa |
| **A44** | | | | | 9.0 ± 2.5 | | |
| **A45** | | | | | 9.2 ± 2.9 | | |
| **A46** | 38.1 ± 13.5 | | | | | | |
| **A47** | | | | | | 117 ± 30.0 | |
| **B40** | 30.9 ± 6.4 | | | 24.5 ± 7.4 | 58.8 ± 11.9 | 34.3 ± 9.8 | 16.8 ± 6.4 |
| **B41** | | 154 ± 24.8 | | 123 ± 19.2 | 79.5 ± 12.8 | 10.3 ± 2.8 | 6.2 ± 2.2 |
| **B42** | | | | | | 138 ± 24.1 | |
| **B46** | 39.7 ± 9.2 | | 69.2 ± 17.2 | | | | |
| **B47** | | | 36.5 ± 14.4 | | | | |
| **C40** | | | 65.8 ± 24.3 | | | 21.8 ± 3.3 | |
| **C41** | | | | 86.0 ± 17.4 | | | |
| **C43** | | | | 249 ± 92.6 | | 77.6 ± 1.1 | |
| **C45** | | | | 2.3 ± 0.6 | | | |
| **C47** | 15.6 ± 4.0 | | | 29.4 ± 9.0 | 24.3 ± 8.1 | 61.5 ± 27.1 | 49.9 ± 18.4 |

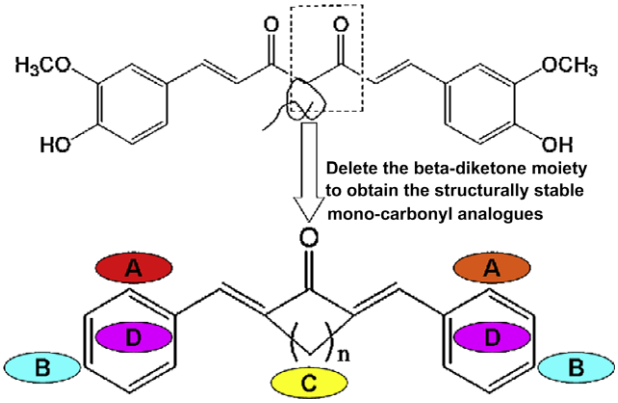


**Figure 5.** The SAR conclusion of mono-carbonyl analogues of curcumin from present data. (A) A strong electron-withdrawing substituent in 2′-position may increase bioactivity and the more electronegative is the moiety, the more cytotoxic is the compound. (B) A weak electron-donating substituent in 4′-position is most favorable to the anti-tumor activity of compound, a strong electron-donating moiety may remove the bioactivity and a strong electron-withdrawing one may reduce it. (C) The acetone and cyclohexanone spacers are much more favorable than the cyclopentanone one. (D) The introduction of heteroaromatic ring is also pharmacologically accessible.

the displacement of a benzene ring by a heteroaromatic ring could maintain or even enhance the cytotoxic activities of mono-carbonyl analogues. It is suggested, therefore, that five-carbon linker analogues of curcumin, which are synthetically accessible may be both pharmacokinetically and pharmacologically favorable for curcumin-based anti-tumor drug development. Our data also provide a few novel leading compounds for the development of structurally stable mono-carbonyl analogues of curcumin.

## 4. Experimental

### 4.1. Chemical synthesis

Melting points were determined on a Fisher-Johns melting apparatus and were uncorrected. $^1$H NMR spectra were recorded on a Varian INOVA-400 spectrometer. The chemical shifts were presented in terms of parts per million with TMS as the internal reference. Electron-spray ionization mass spectra in positive mode (ESI-MS) data were recorded on a Bruker Esquire 3000+ spectrometer. Column chromatography purifications were carried out on Silica Gel 60 (E. Merck, 70–230 mesh). The synthesis and spectral properties of compounds **1**–**3**, **7**–**11**, **13**–**16**, **25**, **30**, **31**, **33**, **40**, and **47** were reported in our previous papers.[22,23] The general procedure of synthesis of **4**–**6**, **12**, **17**–**19**, **32**, **33**–**35**, and **41**–**46** is described as following. An amount of 7.5 mmol acetone (**B**-class), cyclopentanone (**A** class), or cyclohexanone (**C**-class) was added to a solution of 15 mmol arylaldehyde in MeOH (10 ml). The solution was stirred at room temperature for 20 min, followed by dropwise addition of $NaOCH_3/CH_3OH$ (1.5 ml, 7.5 mmol). The mixture was stirred at room temperature and monitored with TLC. When the reaction was finished, the residue was poured into saturated $NH_4Cl$ solution and filtered. The precipitate was washed with water and cold ethanol, and dried in vacuum. The solid was purified by chromatography over silica gel using $CH_2Cl_2/CH_3OH$ as the eluent to yield compounds.

#### 4.1.1. (2*E*,5*E*)-2,5-Bis(2,3-dimethoxybenzylidene)cyclopentanone (A4)

Yellow powder, 66.9% yield, mp 142 °C. $^1$H NMR ($CDCl_3$) $\delta$ = 3.02 (4H, s, $CH_2$–$CH_2$), 3.99 (12H, s, O–$CH_3$ × 4), 6.96 (2H, d, $J$ = 8 Hz, Ar–$H^6$ × 2), 7.11 (2H, t, $J$ = 7.8 Hz, Ar–$H^5$ × 2), 7.18 (2H, d, $J$ = 7.6 Hz, Ar–$H^4$ × 2), 7.93 (2H, s, CH=C × 2). ESI-MS $m/z$: 381.29 $(M+1)^+$, calcd for $C_{23}H_{24}O_5$: 380.4.

#### 4.1.2. (2*E*,5*E*)-2,5-Bis(2-methoxybenzylidene)cyclopentanone (A6)

Yellow powder, 88.7% yield, mp 150–152 °C [155 °C, lit.[30]].

#### 4.1.3. (2*E*,5*E*)-2,5-Bis(3-(allyloxy)-4-methoxybenzylidene)-cyclopenta-none (A12)

Yellow powder, 53.8% yield, mp 129–130 °C. $^1$H NMR ($CDCl_3$) $\delta$ = 3.09 (4H, s, $CH_2$–$CH_2$), 3.93 (6H, s, O–$CH_3$ × 2), 4.67 (4H, t, $J$ = 4.2 Hz, O–$CH_2$ × 2), 5.33 (2H, dd, $J$ = 9.2 Hz, $CH_2^{\alpha}$=C × 2), 5.45 (2H, dd, $J$ = 16 Hz, $CH_2^{\beta}$=C × 2), 6.11 (2H, m), 6.95 (2H, d, $J$ = 8.4 Hz, Ar–$H^6$ × 2), 7.16 (2H, s, Ar–$H^2$ × 2), 7.24 (2H, d, $J$ = 8.4 Hz, Ar–$H^5$ × 2), 7.62 (2H, s, CH=C × 2). ESI-MS $m/z$: 430.41 $(M-1)^+$, calcd for $C_{27}H_{28}O_5$: 432.51.

#### 4.1.4. (2*E*,5*E*)-2,5-Bis(2,5-dimethylbenzylidene)cyclopentanone (A17)

Yellow powder, 81.4% yield, mp 141–143 °C. $^1$H NMR ($CDCl_3$) $\delta$ = 2.36 (6H, s, $Ar^5$–$CH_3$ × 2), 2.41 (6H, s, $Ar^2$–$CH_3$ × 2), 3.00 (4H, s, C–$CH_2$ × 2), 7.08 (2H, d, $J$ = 8 Hz, Ar–$H_3$ × 2), 7.14 (2H, d, $J$ = 8 Hz, Ar–$H_4$ × 2), 7.30 (2H, s, Ar–$H_6$ × 2), 7.79 (2H, s, CH=C × 2). ESI-MS $m/z$: 318.34 $(M-1)^+$, calcd for $C_{23}H_{28}O$: 320.47.

#### 4.1.5. (2*E*,5*E*)-2,5-Bis(4-*tert*-butylbenzylidene)cyclopentanone (A18)

Yellow powder, 61.9% yield, mp 186–188 °C. $^1$H NMR ($CDCl_3$) $\delta$ = 1.35 (18H, s, C–$CH_3$ × 6), 3.11 (4H, s, $CH_2$–$CH_2$), 7.47 (4H, d, $J$ = 8.4 Hz, Ar–$H_{2,6}$ × 2), 7.56 (4H, d, $J$ = 8.4 Hz, Ar–$H_{3,5}$ × 2), 7.59 (2H, s, CH=C × 2). ESI-MS $m/z$: 373.17 $(M+1)^+$, calcd for $C_{27}H_{32}O$: 372.54.

#### 4.1.6. (2*E*,5*E*)-2,5-Bis(4-*tert*-butoxybenzylidene)cyclo-pentanone (A19)

Yellow powder, 74.5% yield, mp 219–220 °C. $^1$H NMR ($CDCl_3$) $\delta$ = 1.40 (18H, s, C–$CH_3$ × 6), 3.10 (4H, s, $CH_2$–$CH_2$), 7.05 (4H, d, $J$ = 8.8 Hz, Ar–$H_{2,6}$ × 2), 7.53 (4H, d, $J$ = 8.8 Hz, Ar–$H_{3,5}$ × 2), 7.57 (2H, s, CH=C × 2). ESI-MS $m/z$: 404.17 $(M^+)$, calcd for $C_{27}H_{32}O_3$: 404.54.

#### 4.1.7. (2*E*,5*E*)-2,5-Bis(2-fluorobenzylidene)cyclopentanone (A32)

Yellow powder, 91.0% yield, mp 207–209 °C. $^1$H NMR ($CDCl_3$) $\delta$ = 3.05 (4H, s, $CH_2$–$CH_2$), 7.09–7.22 (4H, m, Ar–H), 7.38 (2H, m, Ar–H), 7.58 (2H, m, Ar–H), 7.82 (2H, s, CH=C × 2). ESI-MS $m/z$: 297.10 $(M+1)^+$, calcd for $C_{19}H_{14}F_2O$: 296.31.

#### 4.1.8. (2*E*,5*E*)-2,5-Bis(2-chlorobenzylidene)cyclopentanone (A34)

Yellow powder, 87.5% yield, mp 155–158 °C [150–152 °C, lit.[31]].

#### 4.1.9. (2*E*,5*E*)-2,5-Bis(2-(trifluoromethyl)benzylidene)cyclo-penta-none (A35)

Yellow powder, 79.4% yield, mp 90–91 °C. $^1$H NMR ($CDCl_3$) $\delta$ = 2.93 (4H, s, $CH_2$–$CH_2$), 7.45 (2H, m, Ar–H), 7.54 (4H, m, Ar–H), 7.74 (2H, m, Ar–H), 7.88 (2H, s, CH=C × 2). ESI-MS $m/z$: 397.87 $(M+1)^+$, calcd for $C_{21}H_{14}F_6O$: 396.33.

#### 4.1.10. (2*E*,5*E*)-2,5-Bis(thiophen-2-ylmethylene)cyclopenta-none (A41)

Yellow powder, 80.1% yield, mp 222–223 °C [226 °C, lit.[31]].

#### 4.1.11. (2*E*,5*E*)-2,5-Bis((3-methylthiophen-2-yl)methylene) cyclopenta-none (A42)

Yellow powder, 61.7% yield, mp 230–232 °C. $^1$H NMR ($CDCl_3$) $\delta$ = 2.46 (6H, s, $CH_3$ × 2), 3.03 (4H, s, $CH_2$-$CH_2$), 7.00 (2H, d, $J$ = 5.2 Hz, 4′-H × 2), 7.48 (2H, d, $J$ = 5.2 Hz, 5′-H × 2), 7.87 (2H, s, CH=C × 2). ESI-MS $m/z$: 300.26 $(M^+)$, calcd for $C_{17}H_{16}OS_2$: 300.44.

#### 4.1.12. (2*E*,5*E*)-2,5-Bis((5-methylthiophen-2-yl)methylene) cyclopenta-none (A43)

Yellow powder, 56.4% yield, mp 196–199 °C. $^1$H NMR ($CDCl_3$) $\delta$ = 2.56 (6H, s, $CH_3$ × 2), 2.97 (4H, s, $CH_2$–$CH_2$), 6.83 (2H, d, $J$ = 3.6 Hz, 3′-H × 2), 7.20 (2H, d, $J$ = 3.6 Hz, 4′-H × 2), 7.69 (2H, s, CH=C × 2). ESI-MS $m/z$: 301.05 $(M+1)^+$, calcd for $C_{17}H_{16}OS_2$: 300.44.

#### 4.1.13. (2*E*,5*E*)-2,5-Bis((1-methyl-1H-pyrrol-2-yl)methylene) cyclo-pentanone (A45)

Yellow powder, 92.2% yield, mp >250 °C. $^1$H NMR ($CDCl_3$) $\delta$ = 2.92 (4H, s, $CH_2$–$CH_2$), 3.79 (6H, s, N–$CH_3$ × 2), 6.29 (2H, t, $J$ = 2.6 Hz, 4′-H × 2), 6.62 (2H, d, $J$ = 3.6 Hz, 3′-H × 2), 6.84 (2H, s, 5′-H × 2), 7.53 (2H, s, CH=C × 2). ESI-MS $m/z$: 267.64 $(M+1)^+$, calcd for $C_{17}H_{18}N_2O$: 266.34.

#### 4.1.14. (1*E*,4*E*)-1,5-Bis(2,3-dimethoxyphenyl)penta-1,4-dien-3-one (B4)

Yellow powder, 71.2% yield, mp 118–120 °C [108 °C, lit.[30]].

#### 4.1.15. (1*E*,4*E*)-1,5-Di(benzo[*d*][1,3]dioxol-5-yl)penta-1,4-dien-3-one (B5)

Yellow powder, 55.3% yield, mp 182–183 °C [178 °C, lit.[32]].

#### 4.1.16. (1*E*,4*E*)-1,5-Bis(2-methoxyphenyl)penta-1,4-dien-3-one (B6)

Yellow powder, 92.8% yield, mp 118–120 °C [120–122 °C, lit.[33]].

#### 4.1.17. (1*E*,4*E*)-1,5-Bis(2,5-dimethylphenyl)penta-1,4-dien-3-one (B17)

Yellow powder, 93.4% yield, mp 140–142 °C. $^1$H NMR ($CDCl_3$) $\delta$ = 2.36 (6H, s, $Ar^5$–$CH_3$ × 2), 2.44 (6H, s, $Ar^2$–$CH_3$ × 2), 7.00 (2H, d, $J$ = 16 Hz, CO–CH × 2), 7.12 (4H, s, Ar–$H_{3,6}$ × 2), 7.47 (2H, s, Ar–$H_4$ × 2), 8.00 (2H, d, $J$ = 16 Hz, CH=C × 2). ESI-MS $m/z$: 294.70 $(M^+)$, calcd for $C_{21}H_{26}O$: 294.43.

#### 4.1.18. (1*E*,4*E*)-1,5-Bis(4-*tert*-butylphenyl)penta-1,4-dien-3-one (B18)

Yellow powder, 67.0% yield, mp 139–140 °C. $^1$H NMR ($CDCl_3$) $\delta$ = 1.34 (18H, s, C–$CH_3$ × 6), 7.06 (2H, d, $J$ = 16 Hz, CO–CH × 2), 7.44 (4H, d, $J$ = 8 Hz, Ar–$H_{2,6}$ × 2), 7.56 (4H, d, $J$ = 8 Hz, Ar–$H_{3,5}$ × 2), 7.73 (2H, d, $J$ = 16 Hz, CH=C × 2). ESI-MS $m/z$: 347.98 $(M+1)^+$, calcd for $C_{25}H_{30}O$: 346.50.

#### 4.1.19. (1*E*,4*E*)-1,5-Bis(2-(trifluoromethyl)phenyl)penta-1,4-dien-3-one (B35)

Yellow powder, 76.6% yield, mp 131–132 °C [131–133 °C, lit.[31]].

#### 4.1.20. (1*E*,4*E*)-1,5-Di(thiophen-2-yl)penta-1,4-dien-3-one (B41)

Yellow powder, 43.1% yield, mp 118–120 °C [115–117 °C, lit.[34]].

#### 4.1.21. (1*E*,4*E*)-1,5-Bis(3-methylthiophen-2-yl)penta-1,4-dien-3-one (B42)

Yellow powder, 55.9% yield, mp 148–150 °C. $^1$H NMR ($CDCl_3$) $\delta$ = 2.39 (6H, s, $CH_3$ × 2), 6.74 (2H, d, $J$ = 15.2 Hz, CO–$CH_3$ × 2), 7.90 (2H, d, $J$ = 4.8 Hz, 4′-H × 2), 7.28 (2H, d, $J$ = 4.8 Hz, 5′-H × 2), 7.92 (2H, d, $J$ = 15.2 Hz, CH=C × 2). ESI-MS $m/z$: 275.23 $(M+1)^+$, calcd for $C_{15}H_{14}OS_2$: 274.40.

#### 4.1.22. (2*E*,6*E*)-2,6-bis(benzo[*d*][1,3]dioxol-5-ylmethylene) cyclohexa-none (C5)

Yellow powder, 71.1% yield, mp 180–182 °C [189–190 °C, lit.[33]].

#### 4.1.23. 2,6-Bis(2,5-dimethylbenzyl)cyclohexanone (C17)

Yellow powder, 86.5% yield, mp 137–138 °C. $^1$H NMR ($CDCl_3$) $\delta$ = 1.71 (2H, dd, $J$ = 8.0 Hz, $CH_2$), 2.29 (6H, s, $Ar^5$–$CH_3$ × 2), 2.34

(6H, s, $Ar^2$–$CH_3 \times 2$), 2.76 (4H, t, $J = 7.6$ Hz, C–$CH_2 \times 2$), 7.05 (2H, d, $J = 7.6$ Hz, Ar–$H^3 \times 2$), 7.06 (2H, s, Ar–$H^6 \times 2$), 7.12 (2H, d, $J = 7.6$ Hz, Ar–$H^4 \times 2$), 7.87 (2H, s, CH=C × 2). ESI-MS *m/z*: 334.78 ($M^+$), calcd for $C_{24}H_{30}O$: 334.49.

#### 4.1.24. (2*E*,5*E*)-2,5-Bis(2-fluorobenzylidene)cyclopentanone (C32)

Yellow powder, 93.1% yield, mp 100–102 °C. $^1H$ NMR ($CDCl_3$) $\delta = 1.79$ (2H, m), 2.81 (4H, t, $J = 5.8$ Hz, $CH_2$–$CH_2$), 7.07–7.17 (4H, m, Ar–H), 7.31–7.40 (4H, m, Ar–H), 7.83 (2H, s, CH=C × 2). ESI-MS *m/z*: 311.70 $(M+1)^+$, calcd for $C_{20}H_{16}F_2O$: 310.35.

#### 4.1.25. (2*E*,6*E*)-2,6-Bis(2-chlorobenzylidene)cyclohexanone (C34)

Yellow powder, 92.0% yield, mp 94–95 °C. $^1H$ NMR ($CDCl_3$) $\delta = 1.76$ (2H, m), 2.78 (4H, t, $J = 6$ Hz, $CH_2$–$CH_2$), 7.27 (4H, m, Ar–H), 7.33 (2H, m, Ar–H), 7.45 (2H, m, Ar–H), 7.91 (2H, s, CH=C × 2). ESI-MS *m/z*: 344.17 $(M+1)^+$, calcd for $C_{20}H_{26}Cl_2O$: 343.26.

#### 4.1.26. (2*E*,6*E*)-2,6-Bis(2-(trifluoromethyl)benzylidene) cyclohexanone (C35)

Yellow powder, 66.7% yield, mp 107–108 °C. $^1H$ NMR ($CDCl_3$) $\delta = 1.72$ (2H, m), 2.63 (4H, t, $J = 5.2$ Hz, $CH_2$–$CH_2$), 7.33 (2H, d, $J = 7.2$ Hz, Ar–$H^6 \times 2$), 7.44 (2H, t, $J = 7.6$ Hz, Ar–$H^4 \times 2$), 7.55 (2H, t, $J = 7.4$ Hz, Ar–$H^5 \times 2$), 7.71 (2H, d, $J = 7.6$ Hz, Ar–$H^3 \times 2$), 7.96 (2H, s, CH=C × 2). ESI-MS *m/z*: 411.77 $(M+1)^+$, calcd for $C_{22}H_{16}F_6O$: 410.37.

#### 4.1.27. (2*E*,6*E*)-2,6-Bis((5-methylthiophen-2-yl)methylene) cyclohexa-none (C43)

Yellow powder, 71.9% yield, mp 165–167 °C. $^1H$ NMR ($CDCl_3$) $\delta = 1.93$ (2H, m), 2.54 (6H, s, $CH_3 \times 2$), 2.88 (4H, t, $J = 4.8$ Hz, $CH_2$–$CH_2$), 6.80 (2H, d, $J = 3.6$ Hz, 3′-H × 2), 7.18 (2H, d, $J = 3.6$ Hz, 4′-H × 2), 7.89 (2H, s, CH=C × 2). ESI-MS *m/z*: 315.96 $(M+1)^+$, calcd for $C_{18}H_{18}OS_2$: 314.46.

#### 4.1.28. (2*E*,6*E*)-2,6-Bis((1-methyl-1H-pyrrol-2-yl)methylene) cyclo-hexanone (C45)

Yellow powder, 59.6% yield, mp 172–173 °C. $^1H$ NMR ($CDCl_3$) $\delta = 1.89$ (2H, m), 2.85 (4H, t, $J = 5.6$ Hz, $CH_2$–$CH_2$), 3.76 (6H, s, N–$CH_3 \times 2$), 6.26 (2H, t, $J = 3.6$ Hz, 4′-H × 2), 6.57 (2H, d, $J = 3.6$ Hz, 3′-H × 2), 6.82 (2H, s, 5′-H × 2), 7.80 (2H, s, CH=C × 2). ESI-MS *m/z*: 381.23 $(M+1)^+$, calcd for $C_{18}H_{20}N_2O$: 280.36.

### 4.2. Hydrolytic stability

An Agilent 1100 HPLC system equipped with a Hypersil ODS2 column (5 μm × 4.6 mm × 200 mm) was used in this study. The hydrolytic stabilities of the curcumin and analogues were investigated in phosphate-buffered 0.3% (w/v) sodium carboxymethycellulose (CMCNa) solutions at pH 7.4. Two milligrams of samples were weighed accurately and dissolved in 1 ml CMCNa solution by vortex. After stored in the dark at 37 °C for indicated time, the mixture was vortaxed and the sample was analyzed by HPLC. The peak areas were recorded and the degradation rate was calculated by the following formulation:

$$\text{Degradation rate} = \frac{\text{peak area in 0 h} - \text{peak area in 75 h}}{\text{peak area in 0 h}} \times 100\%$$

### 4.3. Pharmacokinetic study in vivo

#### 4.3.1. Chromatographic conditions

An Agilent 1100 HPLC system equipped with a Hypersil ODS2 column (5 μm × 4.6 mm × 200 mm) was used in this study. The mobile phase for curcumin consisted of a mixture of acetonitrile and water (containing 1% HAC) in the ratio 45:55 (v/v) for curcumin, 35:65 (v/v) for **B02**, and 70:30 (v/v) for **B33**. The HPLC system was operated isocratically at a flow rate of 1.0 ml/min and performed at a controlled temperature of 25 °C. Fluorescence detection was performed with excitation and emission wave lengths set at 420 nM (for curcumin), 380 nm (for **B02**), and 320 nm (for **B33**).

#### 4.3.2. Development of HPLC method

The methods used to determine selectivity, standard solution, linearity, sensitivity, precision, and recovery for the establishment of HPLC method were shown in the Supplemental file.

#### 4.3.3. Pharmacokinetic study

The procedures utilized in the animal study were approved by the Wenzhou Medical College Animal Policy and Welfare Committee. Sprague–Dawley male rats with body weights ranging from 160 to 200 g were used for the studies of pharmacokinetics of curcumin and its analogues. All rats were housed in a temperature-controlled room with a 12 h light/dark cycle. 12 rats were randomly divided into three groups: curcumin, **B02**, and **B33**. Compounds, solubilized by the aid of 1% CMCNa, were given orally by gavages with the same dose of 500 mg/kg, respectively. Blood samples (0.5 ml) were obtained from the fossa orbitalis veniplex at 0.083, 0.25, 0.5, 1, 2, 4, and 8 h after administration. After collection, each blood sample was immediately centrifuged for 3 min and the plasma was separated and stored at −20 °C until analysis.

#### 4.3.4. Sample preparation

Samples were determined after extraction by organic solvent. To 400 μl extractant of ethyl acetate/chloroform, 200 μl of plasma was added. The mixture was vortexed for 3 min and centrifuged at 12,000*g* for 5 min, and then the organic phase was transferred to a new vial, dried in vacuum at 40 °C. The dried residue was reconstituted with 100 μl of methanol and vortexed for 1 min. The supernatant was collected and a volume of 20 μl was injected into the HPLC system.

#### 4.3.5. Data analysis

A non-compartmental pharmacokinetic analysis with DAS software was applied to plasma concentration–time data. The pharmacokinetic parameters such as area under the concentration–time curve (AUC), mean residence time (MRT), total clearance (CL/F), and biological half-life ($t_{1/2}$) for each compound were estimated.

## 5. MTT (methyl thiazolyl tetrazolium) assay

Tumor cells were seeded into 96-well plates at a density of 5000 cells per well in 1640 medium, supplemented with 5% heat-inactivated calf serum, 100 U/ml penicillin, and 100 μg/ml streptomycin. The cells were maintained at 37 °C in a humidified atmosphere containing 5% $CO_2$. All experiments were carried out 24 h after cells were seeded. Tested compounds were dissolved in DMSO and diluted with 1640 medium to the final concentrations of 100, 33.3, 11.1, and 3.7 μg/ml. The tumor cells were incubated with test compounds for 72 h before the MTT assay. A fresh solution of MTT (5 mg/ml) prepared in NaCl solution (0.9%) was added to each single well of the 96-well plate. The plate were then incubated in a $CO_2$ incubator for 3 h, cells dissolved with 100 μl DMSO, and then analyzed in a multi-well-plate reader at 570 nM. Cisplatin was applied as positive control.

## Acknowledgments

This work was supported by the National Natural Science Funding of China (20802054), General Grant of Zhejiang Administration of Chinese Traditional Medicine (2007CA080&79 to G.L.), China; The NJUST Innovative Ph.D. Training Project (2007 to G.L.), China; Zhejiang Provincial Program for the Cultivation of High-level Inno-

vative Health talents (to X.K.L.), China. We also thank the Pharmacy College of Zhejiang University for the MTT assay and Dr. Huiping Zhou in Virginia Commonwealth University for the review and revision in English writing.

## Supplementary data

Supplementary data associated with this article can be found, in the online version, at doi:10.1016/j.bmc.2008.10.044.

## References and notes


1. Kuttan, R.; Sudheeran, P. C.; Josph, C. D. *Cancer Lett.* **1985**, *29*, 197.
2. Kuttan, R.; Sudheeran, P. C.; Josph, C. D. *Tumori* **1987**, *73*, 29.
3. NCI, DCPC, *J. Cell Biochem.* **1996**, *26S*, 72.
4. Jagetia, G. C.; Aggarwal, B. B. *J. Clin. Immunol.* **2007**, *27*, 19.
5. Kumar, A. P.; Aggarwal, B. B.; Bharti, A. C. *Anticancer Res.* **2003**, *23*, 363.
6. Chakraborty, S.; Ghosh, U.; Bhattacharyya, N. P. *Mutat. Res.* **2006**, *596*, 81.
7. Huang, M. T.; Lou, Y. R.; Ma, W. *Cancer Res.* **1994**, *54*, 5841.
8. Mukherjee Nee Chakraborty, S.; Ghosh, U.; Bhattacharyya, N. P.; Bhattacharya, R. K.; Dey, S.; Roy, M. *Mol. Cell Biochem.* **2007**, *297*, 31.
9. Pesic, M.; Markovic, J. Z.; Jankovic, D.; Kanazir, S.; Markovic, I. D.; Rakic, L. *J. Chemother.* **2006**, *18*, 66.
10. Hsu, C. H.; Cheng, A. L. *Adv. Exp. Med. Biol.* **2007**, *595*, 471.
11. Pan, M. H.; Huang, T. M.; Lin, J. K. *Drug Metab. Dispos.* **2000**, *27*, 486.
12. Sharma, R. A.; Steward, W. P.; Gescher, A. J. *Adv. Exp. Med. Biol.* **2007**, *595*, 453.
13. Garcea, G.; Jones, D. J.; Singh, R.; Dennison, A. R.; Farmer, P. B.; Sharma, R. A. *Br. J. Cancer* **2004**, *90*, 1011.
14. Todd, P. H. UK Pat. Appl. DE 4026118C2, 1991.
15. Wang, Y. J.; Pan, M. H.; Cheng, A. L.; Lin, L.; Ho, Y. S.; Hsieh, C. Y. *J. Pharm. Biomed. Anal.* **1997**, *15*, 1867.
16. Másson, M.; Tomren, M. A.; Tønnesen, H. H.; Loftsson, T. *Int. J. Pharm.* **2007**, *338*, 27.
17. Straganz, G. D.; Glieder, A.; Brecker, L.; Ribbons, D. W.; Steiner, W. *Biochem. J.* **2003**, *369*, 573.
18. Rosemond, M. J.; St. John-Williams, L.; Yamaguchi, T.; Fujishita, T.; Walsh, J. S. *Chem. Biol. Interact.* **2004**, *147*, 129.
19. Grogan, G. *Biochem. J.* **2005**, *388*, 721.
20. Robinson, T. P.; Ehlers, T.; Hubbard, I. V.; Bai, X.; Arbiser, J. L.; Goldsmith, D. J. *Bioorg. Med. Chem. Lett.* **2003**, *13*, 115.
21. Ohtsu, H.; Xiao, Z.; Ishida, J.; Nagai, M.; Wang, H. K.; Itokawa, H. *J. Med. Chem.* **2002**, *45*, 5037.
22. Liang, G.; Yang, S.; Jiang, L.; Zhao, Y.; Shao, L.; Xiao, J. *Chem. Pharm. Bull.* **2008**, *56*, 162.
23. Liang, G.; Li, X.; Chen, L.; Yang, S.; Wu, X.; Studer, E. *Bioorg. Med. Chem. Lett.* **2008**, *18*, 1525.
24. Liang, G.; Yang, S.; Xiao, J. *Eur. J. Med. Chem.* **2008**. doi:10.1016/j.ejmech.2008.01.031.
25. Jovanovic, S. V.; Boone, C. W.; Steenken, S.; Trinoga, M.; Kaskey, R. B. *J. Am. Chem. Soc.* **2001**, *123*, 3064.
26. Litwinienko, G.; Ingold, K. U. *J. Org. Chem.* **2004**, *69*, 5888.
27. Woo, H. B.; Shin, W. S.; Lee, S.; Ahn, C. M. *Bioorg. Med. Chem. Lett.* **2005**, *15*, 3782.
28. Lin, L.; Shi, Q.; Nyarko, A. K.; Bastow, K. F.; Wu, C. C.; Su, C. Y. *J. Med. Chem.* **2006**, *49*, 3963.
29. Thangapazha, R. L.; Sharma, A.; Maheshwari, R. K. *AAPS J.* **2006**, *8*, E443.
30. Weber, W. M.; Hunsaker, L. A.; Abcouwer, S. F.; Deck, L. M.; Vander Jagt, D. L. *Bioorg. Med. Chem.* **2005**, *13*, 3811.
31. Weber, W. M.; Hunsaker, L. A.; Roybal, C. N.; Bobrovnikova-Marjon, E. V.; Abcouwer, S. F.; Royer, R. E. *Bioorg. Med. Chem.* **2006**, *14*, 2450.
32. Brahmbhatt, D. I.; Pandya, U. R. *Indian J. Chem. B: Org. Chem. Med. Chem.* **2003**, *42B*, 145.
33. Adams, B. K.; Ferstl, E. M.; Davis, M. C.; Herold, M.; Kurtkaya, S.; Camalier, R. F. *Bioorg. Med. Chem.* **2004**, *12*, 3871.
34. Weber, W. M.; Hunsaker, L. A.; Gonzales, A. M.; Heynekamp, J. J.; Orlando, R. A.; Deck, L. M. *Biochem. Pharmacol.* **2006**, *72*, 928.